J. Synchrotron Rad. (1997). **4**, 47–53

A Method to Provide Magnet-Free Long Straight Sections in Low-Emittance Synchrotron Radiation Sources

Hitoshi Tanaka,* Kouichi Soutome and Masahiro Hara

SPring-8, JASRI-JAERI-RIKEN Project Team, Kamigori, Ako-gun, Hyogo 678-12, Japan. E-mail: tanaka@spring8.or.jp

(*Received 22 October 1996; accepted 20 December 1996*)

In a low-emittance synchrotron radiation source it is difficult to provide magnet-free long straight sections (MLSSs) a few tens of metres long because introducing MLSSs to the radiation source causes symmetry breaking and markedly reduces dynamic stability. To overcome this difficulty and realize MLSSs in such a ring, a method of building MLSSs is proposed starting from the stable lattice with high symmetry and proceeding *via* a transient lattice.

Keywords: long straight sections; high brilliance; low-emittance storage rings; dynamic aperture; machine lattice.

1. Introduction

Installation of magnet-free long straight sections (MLSSs) a few tens of metres long in a low-emittance synchrotron radiation source has been studied at some new synchrotron radiation facilities (Kamitsubo, 1991; Brunelle *et al.*, 1994; Joho, Marchand, Rivkin & Streun, 1994; Kamiya *et al.*, 1994). MLSSs are expected to open the possibilities of achieving more brilliant photon beams by increasing the number of undulator periods and of developing or installing special devices such as free-electron lasers that can provide coherent synchrotron radiation.

On the other hand, as described below, it is difficult to introduce MLSSs into low-emittance synchrotron radiation sources. Among such radiation sources, the so-called third-generation synchrotron radiation sources are characterized by their small dynamic apertures due to strong sextupoles. When MLSSs are introduced, new harmful resonances appear near an operation point owing to symmetry breaking of the optics. Hence, the introduction of MLSSs generally reduces the dynamic stability of the ring and also makes it more sensitive to magnetic errors. It is therefore important when introducing MLSSs to optimize the lattice design and to commission the ring to overcome such poor stability.

Recently, some lattice designs with sufficient stability have been presented (Brunelle *et al.*, 1994; Takaki, Kobayashi, Matsuda & Kamiya, 1995; Kaltchev, Servranckx, Craddock & Joho, 1995). The lattice parameters were successfully optimized by taking advantage of mirror symmetry on resonance suppression, reasonable optical matching, and so on. In particular, work performed by the LURE and LNS group (Brunelle *et al.*, 1994) provided a method of optimizing the lattice with the MLSSs whereby unit transfer matrices are used to preserve the suppression of systematic resonances in each regular cell.

In this paper we present a different method of constructing MLSSs in a low-emittance synchrotron radiation source *via* a three-stage procedure. This enables us to provide MLSSs efficiently because our method, described below, needs only simple optical matching (or small matching sections) compared with the matching of Brunelle *et al.* (1994). In the first stage the ring is commissioned using a stable lattice called a 'phase I lattice'. The features of this lattice are high symmetry to keep dynamic stability and the phase advance of a horizontal betatron oscillation which is related to that of the final 'phase II lattice' with the MLSSs. By using information on the closed-orbit distortion (COD) correction for the phase I lattice, the MLSSs are built *via* the 'transient lattice' with the same horizontal and vertical tunes as those of the phase II lattice. Hereafter, we call this the 'three-stage commissioning' (TSC) method.

Utilization of the radiation source is thus divided into two phases by the operating lattice configuration. During phase I, only standard straight sections several metres long are available for users. On the other hand, in phase II both standard and long straight sections are available. It should be stressed here that phase I can be linked quickly and easily to phase II by the TSC method. In the following section, four key concepts of our method are explained from the viewpoint of beam dynamics. Then, in §3, a procedure for providing MLSSs is described in detail. In §4, simulation results are shown for the case of the SPring-8 storage ring (Kamitsubo, 1991) as an example application.

2. Key concepts

The TSC method can be considered as commissioning with a series of detuned lattices (Tsumaki, Nagaoka, Tanaka, Yoshida & Hara, 1989) composed of three stages which are sequentially linked *via* information on the COD correction. To use the TSC method effectively, the following four concepts are essential.

2.1. *Introduction of missing bending-magnet cells (straight cells)*

To produce MLSSs easily, bending magnets in the phase I lattice are removed initially from each of the unit cells in which an MLSS is to be built. Since a low-emittance radiation source needs a small deflection angle, θ_b, of a bending magnet (Sommer, 1983; Kamiya & Kihara, 1983; Teng, 1985), the focusing force of a bending magnet, which is approximately proportional to θ_b, is weak compared with that of a quadrupole magnet. Therefore, the symmetry of the optics is scarcely broken by only removing bending magnets from a few unit cells. This is important for both easy commissioning of the phase II lattice and keeping the dynamic stability of the phase I and the transient lattices.

2.2. *Optics and phase matching*

When the lattice of a ring is partly modified, information on the COD correction for the previous ring (before modification) cannot be applied to the modified ring without following two kinds of matching. (i) All optical functions, *i.e.* betatron, alpha (derivative of a betatron function by path length s) and dispersion functions in each modified part are matched to those in unmodified parts at both ends. This means that the distribution of each optical function is kept completely unchanged in the unmodified parts of the ring. (ii) The difference between phase advances of a horizontal betatron oscillation in the two lattices before and after modification is matched to a multiple of 2π (see Appendix *A*).

The former is called 'optics matching' and the latter 'phase matching'. Both assure that the propagation of a single kick of any steering magnet in unmodified parts of the ring is not affected by the modification. In (ii), only the horizontal phase advance is taken into account because the horizontal COD dominates over dynamic stability in a low-emittance synchrotron radiation source.

2.3. *Localization of COD sources*

When the horizontal COD is induced, circulating beams are subjected to extra quadrupole fields at all sextupoles, each having a magnitude that is proportional to the COD at that point. These quadrupole error fields distort betatron functions along the ring and consequently induce accidental linear and non-linear resonances.

In the case where the horizontal COD is generated by a 'single kick', a main harmonic of the COD, N_{ν_x} corresponds to the tune of a horizontal betatron oscillation. This kind of COD causes the distortion of a horizontal (vertical) betatron function which has the main harmonics of $N_{\nu_x} \pm N_s$ ($N_{\nu_x} - 2N_{\nu_y} \pm N_s$) and $3N_{\nu_x} \pm N_s$ ($N_{\nu_x} + 2N_{\nu_y} \pm N_s$), where N_s is the super-periodicity of a ring (see Appendix *B*). Provided that harmful structure resonances due to sextupoles are suppressed by optimizing the strength of sextupoles, both the linear and non-linear accidental resonances excited reflect the harmonics of the betatron distortion. Therefore, the resonances close to an operation point are not easily excited by this kind of COD. As the number of random error sources is increased, in general, the spectra of both the COD and the distortion of the betatron functions become wider. This means that the accidental resonances around an operation point are more excited compared with the single-kick case. Hence, to keep the dynamic stability of the ring with a COD of a few millimeters it is important to decrease the COD sources in the ring, *i.e.* to make the COD pseudo-periodic as in the single-kick case.

2.4. *No sextupole magnet in modified sections*

The dynamic aperture is determined by the strength distribution of sextupoles. In the case where no sextupole exists in each modified section and the two kinds of matching are performed there, the dynamic aperture never depends on the optics of the modified sections. This concept makes both the optimization of sextupole strength and the optics design of modified sections easy by separating them.

3. Three-stage commissioning method

The TSC method is schematically shown in Fig. 1. Details of each stage are described below.

3.1. *Stage 1: commissioning with the phase I lattice*

At first, the ring is commissioned by using the phase I lattice composed of a number of unit cells and a small

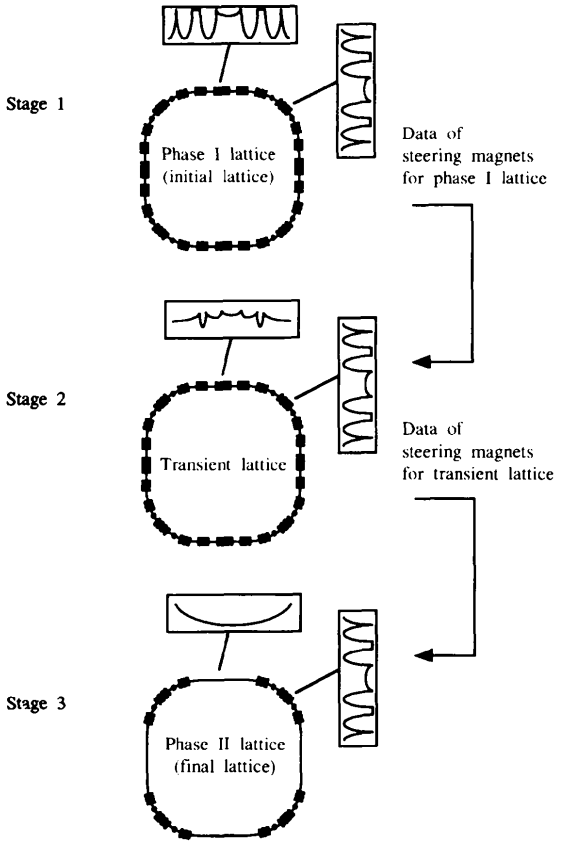

Figure 1
Schematic diagram of the construction of MLSSs by the TSC method.

number of straight cells from which the bending magnets have been removed. The phase matching in a horizontal plane and optics matching in both horizontal and vertical planes are taken between the phase I and phase II lattices. The beams are stored by using established procedures such as first-turn steering (Farvacque & Ropert, 1989). At the end of stage 1, the strength distribution of the steering magnets is obtained for the phase I lattice, by which the r.m.s. value of the COD can be reduced to a few tenths of millimetres.

3.2. *Stage 2: machine study with a transient lattice*

Next, by adjusting the strength of quadrupoles and sextupoles in the straight cells, the phase I lattice is converted into a transient lattice. In the transient lattice, the horizontal and vertical tunes are set to be the same as those of the phase II lattice, keeping optics and phase matching. By using the transient lattice, commissioning with the phase II lattice is simulated without magnet rearrangement. In the machine tuning with the transient lattice, the steering-magnet data obtained in stage 1 are used as initial values. No special procedure such as first-turn steering is necessary for beam accumulation owing to two kinds of matching and the localization of COD sources. Through the machine study, the strength distribution of the steering magnets is determined for the transient lattice.

3.3. *Stage 3: commissioning with the phase II lattice*

Finally, the ring is commissioned by using the phase II lattice with the MLSSs, which are constructed by simple rearrangement of magnets in the straight cells. Here, the steering-magnet data obtained in stage 2 are also used as initial values. Since the COD is only excited by the small change of dipole error fields due to the rearrangement, no special procedure is necessary for beam accumulation.

Although stage 2 can be omitted in principle, it is better to perform it in order to confirm that there are no fatal defects in unmodified parts of the ring. When any problems occur in stage 3, the completion of stage 2 ensures that they are caused by the modified or newly installed parts of the ring in stage 3.

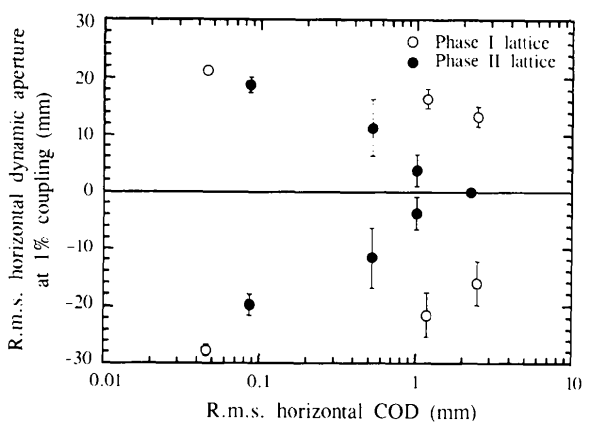

Figure 2
Reduction of the dynamic aperture against the r.m.s. horizontal COD. The empty and filled circles denote commissioning of the phase I and phase II lattices, respectively, by a single step. Error bars represent one standard deviation.

Table 1
R.m.s. errors assumed in the simulation.

Error item	R.m.s. value
Monitoring error	
First-turn measurement (mm)	1
Multiturn (normal COD) measurement (mm)	0.1
Injection error	
Position stability (mm)	1
Angle stability (mrad)	0.1
Magnet misalignment†	
Girder (mm)	0.2
Magnets within a girder (mm)	0.05
Magnet field error ratio/tilt error‡ (mrad)	
Bending	5×10^{-4}/0.1
Quadrupole	5×10^{-4}/0.2
Sextupole	1×10^{-3}/0.5

† The two-stage magnet alignment method (Tanaka, Kumagai & Tsumaki, 1992) is assumed. ‡ The tilt error shows the tilt of a magnet around the longitudinal axis.

4. Construction of MLSSs in the SPring-8 storage ring

The TSC method was adopted for providing four 30 m-long MLSSs in the SPring-8 storage ring. This is because the stability of the phase II lattice is more sensitive to the orbit distortion as described in the previous sections. Fig. 2 shows the reduction of the dynamic aperture against the r.m.s. horizontal COD for two cases: direct commissioning of the phase I and phase II lattices, not using the TSC method. In this simulation, the r.m.s. errors listed in Table 1 are assumed. As seen in Fig. 2 in the region where the r.m.s. COD is a few mm, a dynamic aperture of 10 mm is kept for the phase I lattice but almost vanishes for the phase II lattice. Therefore, the r.m.s. value of the COD should be suppressed to less than 1 mm in order to store the beams at the first stage of commissioning. It appears to be difficult to achieve this by using the first-turn monitoring system because its accuracy is $\sim$1 mm and the injection orbit stability is not better than 1 mm and 0.1 mrad.

The optics and main parameters designed for the TSC method are shown in Fig. 3 and Table 2, respectively. The optics of the SPring-8 storage ring are of a hybrid type where betatron functions become high and low alternately. Four MLSSs are scheduled to be installed with fourfold symmetry, but mirror symmetry is broken due to the hybrid optics. The horizontal phase advance of each MLSS is $\sim 25°$, which is just 2π smaller than that of the straight cell in the phase I lattice. Quadrupole quintets are used at both ends of each MLSS to tailor the optics, keeping the peaks of betatron functions less than 60 m.

By using these parameters, the commissioning procedure has been simulated. Fig. 4 shows the r.m.s. COD against the COD correction phase for ten rings, each of which has a different magnetic error distribution. The correction phase represents the process of the TSC method and is defined as follows: phase 0, the phase I lattice without any correction;

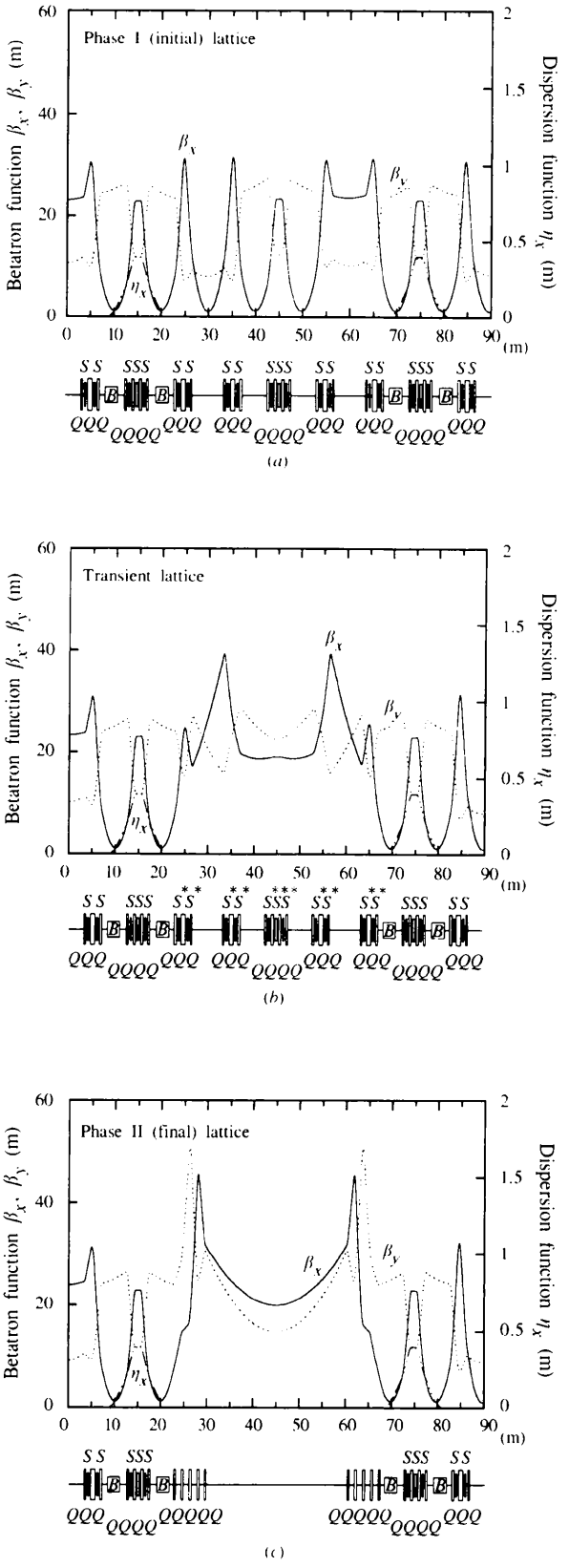

Figure 3
Optics and magnet lattice of three cells of the SPring-8 storage ring. (*a*), (*b*) and (*c*) show the phase I, transient and phase II lattices, respectively. The symbols *S*, *Q* and *B* denote a sextupole, a quadrupole and bending magnets, respectively. The symbol *S** denotes a sextupole magnet turned off.

Table 2
Optics data of the SPring-8 storage ring.

	Phase I	Transient	Phase II
Energy (GeV)	8	8	8
Emittance (nm rad)	7	7	7
Betatron tune			
Horizontal	51.22	47.12	47.12
Vertical	16.16	15.22	15.22
Chromaticity			
Horizontal	−116	−74.7	−77.4
Vertical	−40.0	−27.8	−35.0
Magnet-free straight sections			
Normal (6.65 m)	48	48	44
Long (30 m)	0	0	4

phase 1, the phase I lattice after first-turn steering; phase 2, the phase I lattice after the COD correction; phase 3, the transient lattice with steering magnet strength of the phase I lattice; phase 4, the transient lattice after the COD correction; phase 5, the phase II lattice with steering magnet strength of the transient lattice; phase 6, the phase II lattice after the COD correction. In this simulation, (i) *MICADO* (Autin & Marti, 1973) is used to correct the COD, (ii) the same error condition as listed in Table 1 is also used, and (iii) steering magnets in the straight cells are not used to avoid the calculation for their replacement by other steering magnets. The third condition means the COD generated by each steering magnet in the modified sections is varied along the ring even when both the phase and optics are matched. By using the strength data of steering magnets for

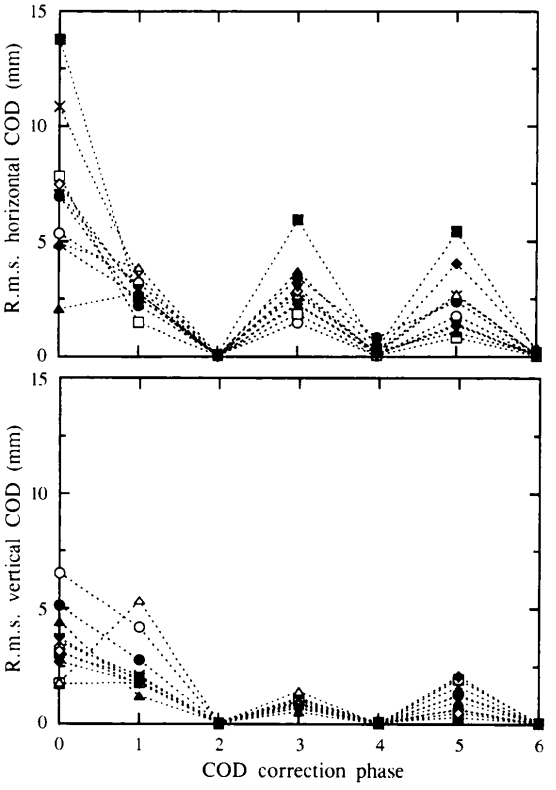

Figure 4
The r.m.s. horizontal and vertical COD against the COD correction phase. The COD correction phases are defined in the text.

the previous lattice as initial values, the r.m.s. COD is kept to less than ~5 mm. In Fig. 4 the vertical COD is also kept small at correction phase 3 even though the vertical phase is not matched. This is because the strength of steering magnets is scattered along the ring through the first-turn steering procedure. This shows that the r.m.s. vertical COD markedly depends on the COD correction scheme up to correction phase 2.

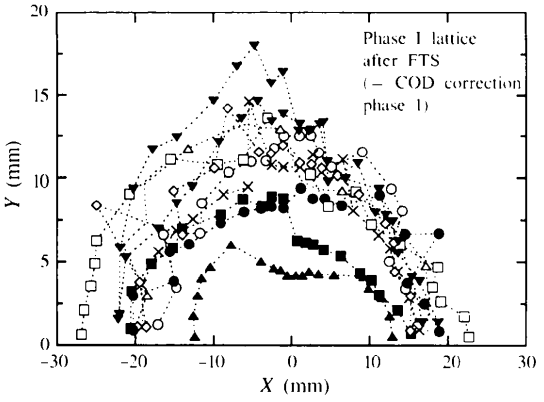

Figure 5
Dynamic aperture of the phase I lattice after first-turn steering. The turn number is 500 and the calculation is performed at the injection point for ten rings, each of which has a different error condition.

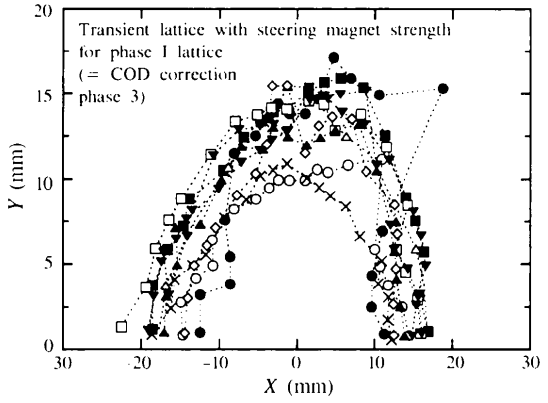

Figure 6
Dynamic aperture of the transient lattice with the steering magnet strength of the phase I lattice. The calculation condition is the same as for Fig. 5.

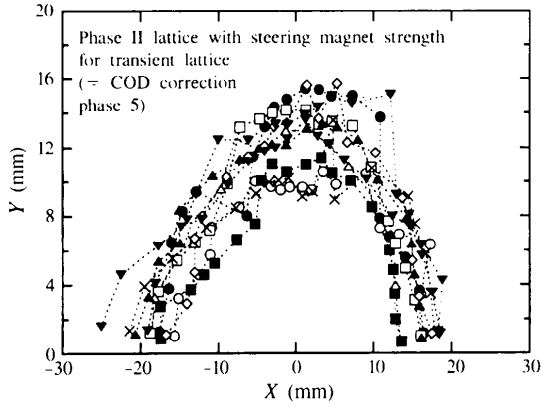

Figure 7
Dynamic aperture of the phase II lattice with the steering magnet strength of the transient lattice. The calculation condition is the same as for Fig. 5.

Figs. 5, 6 and 7 show three kinds of dynamic aperture for correction phases 1, 3 and 5 in Fig. 4, respectively. The same ten rings as shown in Fig. 4 are used for each correction phase. At the beginning of stage 1 (correction phase 1), stage 2 (correction phase 3) and stage 3 (correction phase 5), the horizontal aperture of 10 mm and the vertical aperture of 5 mm are kept at low and high coupling ratios, respectively. These are sufficient for beam injection and for machine tuning.

The case where stage 2 is omitted is also simulated. Here, the strength data of the steering magnets for the phase I lattice are used as the initial values of those for the phase II lattice. The r.m.s. COD and dynamic aperture obtained for the phase II lattice are almost the same as those of the normal TSC case. Fig. 8 shows the dynamic aperture of the phase II lattice for the same ten rings shown in Fig. 4.

5. Summary and discussion

We proposed the TSC method to construct MLSSs a few tens of metres long in a low-emittance synchrotron radiation source. This is based on four concepts which are reasonable from the viewpoint of beam dynamics: (i) introduction of missing bending-magnet cells, (ii) optics and phase matching, (iii) localization of COD sources, and (iv) no sextupole magnet in modified sections. According to the multistage approach, utilization of the radiation source is divided into two phases, phase I and II. Although the MLSSs are not available during phase I, it should be stressed that the TSC method makes standard straight sections available from the beginning of phase I and it also smoothly links these two phases together.

To provide MLSSs, the best way is to optimize the lattice with MLSSs so as to have sufficient stability, not only for a steady operation but also for commissioning. It is apparent, however, that this approach cannot be applied to all cases,

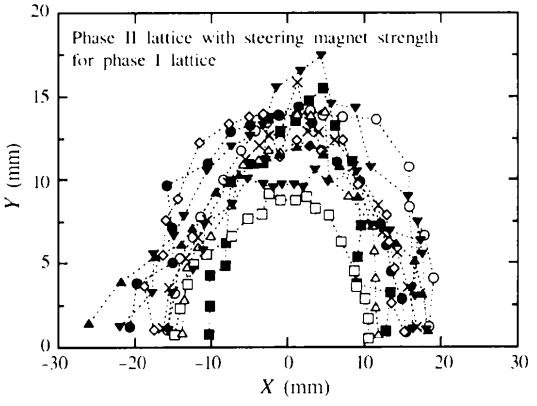

Figure 8
Dynamic aperture of the phase II lattice with the steering magnet strength of the phase I lattice. The calculation condition is the same as for Fig. 5.

especially to third-generation synchrotron radiation sources, which are not stable even without the MLSSs. Even for such a case, there is some possibility of providing MLSSs by the TSC method.

To see the effect of the TSC method on the construction of MLSSs in a ring with poor stability, the problem of constructing MLSSs in the SPring-8 storage ring was investigated. The lattice with four 30 m-long MLSSs is not stable and it is difficult to commission the ring directly. The simulation results show that the TSC method is effective, *i.e.* four MLSSs can be built by the TSC method more easily and safely compared with the case where the lattice with the MLSSs is commissioned directly.

APPENDIX A

Closed-orbit distortion induced by a single dipole kick at the azimuthal position s_1 is given by (Sands, 1970)

$$\begin{aligned} X_z(s) = {} & [\beta_z^{1/2}(s)/2 \sin \pi\nu_z]\beta_z^{1/2}(s_1) \\ & \times \cos [\pi\nu_z - |\mu_z(s) - \mu_z(s_1)|] \\ & \times \Delta B_w L(s_1)/B\rho, \end{aligned}$$

$$\mu_z(s) = \int_{s_0}^{s_0 + s} \mathrm{d}a\,[\beta_z(a)]^{-1}, \qquad (1)$$

where $z = x$, $w = y$ or $z = y$, $w = x$, and where s, $\beta_z(s)$, ν_z, $\Delta B_w L(s_1)$ and $B\rho$ are the azimuthal position, the betatron function, the tune of a betatron oscillation, the integrated dipole field and the magnet rigidity, respectively. The subscripts 0, x and y denote the reference, horizontal and vertical axes, respectively, which are perpendicular to a design orbit. Provided that the phase advance is locally modified by $\Delta\mu_z$ but betatron functions are matched at both ends of a modified section, the COD for an unmodified section is expressed as

$$\begin{aligned} \bar{X}_z(s) = {} & [\beta_z^{1/2}(s)/2 \sin (\pi\nu_z + \Delta\mu_z/2)]\beta_z^{1/2}(s_1) \\ & \times \cos [\pi\nu_z + \Delta\mu_z/2 \pm \alpha - |\mu_z(s) - \mu_z(s_1)|] \\ & \times \Delta B_w L(s_1)/B\rho, \end{aligned} \qquad (2)$$

where $\alpha = 0$ or $\Delta\mu_z$.

To satisfy $\bar{X}_z(s) = X_z(s)$, it is easily found that $\Delta\mu_z$ should be a multiple of 2π.

APPENDIX B

The distortion of a betatron function induced by quadrupole error fields is periodic in one revolution and given by

$$\begin{aligned} \Delta\beta_z(s) = {} & [-\beta_z(s)/2 \sin 2\pi\nu_z] \\ & \times \int_{s_0}^{s_0 + C} \Big\{\beta_z(\bar{s}_1)\Lambda q(\bar{s}_1) \\ & \times \cos 2[\pi\nu_z - |\mu_z(s) - \mu_z(\bar{s}_1)|]\,\mathrm{d}\bar{s}_1\Big\}, \end{aligned} \qquad (3)$$

where $\Lambda = 1$ for $z = x$; $\Lambda = -1$ for $z = y$. $q(s)$ is the normal quadrupole error field at the azimuthal position s, and C is the circumference of a ring. Assuming that the COD is induced by a single horizontal kick and the error fields are caused by the horizontal COD at thin sextupoles, (3) is rewritten using (1) as

$$\begin{aligned} \Delta\beta_z(s) = {} & [-\beta_z(s)/4 \sin \pi\nu_x \sin 2\pi\nu_z] \\ & \times \int_{s_0}^{s_0 + C} \mathrm{d}\bar{s}_2 \Big\{\beta_z^{3/2}(\bar{s}_2)\beta_z^{1/2}(\bar{s}_1)\Lambda\Lambda(\bar{s}_2) \\ & \times [\Delta B_y L(\bar{s}_1)/B\rho] \cos [\pi\nu_x - |\mu_x(\bar{s}_2) - \mu_x(\bar{s}_1)|] \\ & \times \cos 2[\pi\nu_z - |\mu_z(s) - \mu_z(\bar{s}_2)|]\Big\}, \end{aligned} \qquad (4)$$

where

$$\Lambda(s) = \sum_{i=1}^{n_s} (B''_{yi}L_i/B\rho)\delta(s - s_i),$$

$$B''_{yi} = \partial^2 B_{yi}L_i/\partial y^2,$$

and $z = x$, y. In the above equation, $B''_{yi}L_i$, $\delta(s)$ and n_s are the integrated strength of the ith sextupole magnet, the periodic delta function and the number of sextupole magnets, respectively. By setting $s_0 = \bar{s}_1$ and rearranging (4) to reveal characteristic frequencies, we obtain

$$\begin{aligned} \Delta\beta_z(s) = {} & [-\Lambda\beta_z(s)\beta_z^{1/2}(s_0)/4 \sin \pi\nu_x \sin 2\pi\nu_z] \\ & \times \sum_{i=1}^{n_s} (B''_{yi}L_i/B\rho)\beta_{zi}^{3/2}[\Delta B_y L(s_0)/B\rho] \\ & \times \cos (\pi\nu_x - \mu_{xi}) \cos 2[\pi\nu_z - |\mu_z(s) - \mu_z(s_i)|] \\ = {} & -[\Lambda\beta_z(s)\beta_z^{1/2}(s_0)/4 \tan \pi\nu_x \tan 2\pi\nu_z] \\ & \times [\Delta B_y L(s_0)/(B\rho)^2] \\ & \times \sum_{i=1}^{n_s} B''_{yi}L_i\beta_{zi}^{3/2} \cos (\mu_{xi}) \cos 2[\mu_z(s) - \mu_{zi}] \\ & - [\Lambda\beta_z(s)\beta_z^{1/2}(s_0)/4 \tan \pi\nu_x][\Delta B_y L(s_0)/(B\rho)^2] \\ & \times \sum_{i=1}^{n_s} B''_{yi}L_i\bar{\Lambda}_i\beta_{zi}^{3/2} \cos (\mu_{xi}) \sin 2[\mu_z(s) - \mu_{zi}] \\ & - [\Lambda\beta_z(s)\beta_z^{1/2}(s_0)/4 \tan 2\pi\nu_z][\Delta B_y L(s_0)/(B\rho)^2] \\ & \times \sum_{i=1}^{n_s} B''_{yi}L_i\beta_{zi}^{3/2} \sin (\mu_{xi}) \cos 2[\mu_z(s) - \mu_{zi}] \\ & - [\Lambda\beta_z(s)\beta_z^{1/2}(s_0)/4][\Delta B_y L(s_0)/(B\rho)^2] \\ & \times \sum_{i=1}^{n_s} B''_{yi}L_i\bar{\Lambda}_i\beta_{zi}^{3/2} \sin (\mu_{xi}) \sin 2[\mu_z(s) - \mu_{zi}], \end{aligned} \qquad (5)$$

where $\bar{\Lambda}_i = 1$ for $s \geq s_i$; $\bar{\Lambda}_i = -1$ for $s < s_i$, and $z = x$, y. The parameter $\bar{\Lambda}_i$ shows that the phase jumps at the ith quadrupole error field to satisfy a periodic condition. Since the main harmonics of a betatron function and sextupole arrangement are the zeroth (DC) and N_sth components, respectively, where N_s is the super-periodicity of a ring, $\Delta\beta_z(s)$ is approximately expressed by harmonic

components as

$$\begin{aligned}\Delta\beta_z \simeq\ & \bar{A}_1 \cos(2\pi s N_{\nu_x}/C) \\ & \times [\bar{a}_1 \sin(2\pi s N_s/C) + \bar{b}_1 \cos(2\pi s N_s/C)] \\ & \times [\bar{c}_1 \sin(4\pi s N_{\nu_z}/C) + \bar{d}_1 \cos(4\pi s N_{\nu_z}/C)] \\ & + \bar{A}_2 \cos(2\pi s N_{\nu_x}/C) \\ & \times [\bar{a}_1 \sin(2\pi s N_s/C) + \bar{b}_1 \cos(2\pi s N_s/C)] \\ & \times [\bar{c}_2 \sin(4\pi s N_{\nu_z}/C) + \bar{d}_2 \cos(4\pi s N_{\nu_z}/C)] \\ & + \bar{A}_3 \sin(2\pi s N_{\nu_x}/C) \\ & \times [\bar{a}_2 \sin(2\pi s N_s/C) + \bar{b}_2 \cos(2\pi s N_s/C)] \\ & \times [\bar{c}_1 \sin(4\pi s N_{\nu_z}/C) + \bar{d}_1 \cos(4\pi s N_{\nu_z}/C)] \\ & + \bar{A}_4 \sin(2\pi s N_{\nu_x}/C) \\ & \times [\bar{a}_2 \sin(2\pi s N_s/C) + \bar{b}_2 \cos(2\pi s N_s/C)] \\ & \times [\bar{c}_2 \sin(4\pi s N_{\nu_z}/C) + \bar{d}_2 \cos(4\pi s N_{\nu_z}/C)] \\ =\ & A_1 [a_1 \sin(2\pi s N_s/C) + b_1 \cos(2\pi s N_s/C)] \\ & \times [a_2 \sin(2\pi s N_{\nu_x}/C) + b_2 \cos(2\pi s N_{\nu_x}/C)] \\ & \times [a_3 \sin(4\pi s N_{\nu_z}/C) + b_3 \cos(4\pi s N_{\nu_z}/C)], \quad (6)\end{aligned}$$

where $z = x$, y, and $\bar{A}_{1\text{-}4}$, $a_{1\text{-}3}$, $b_{1\text{-}3}$, $\bar{a}_{1\text{-}2}$ $\bar{b}_{1\text{-}2}$, $\bar{c}_{1\text{-}2}$, $\bar{d}_{1\text{-}2}$ and A_1 are constants and N_{ν_z} is the harmonic of a betatron oscillation. From (6) it is found that the horizontal (vertical) betatron distortion has main harmonics of $N_{\nu_x} \pm N_s$ ($N_{\nu_x} - 2N_{\nu_y} \pm N_s$) and $3N_{\nu_x} \pm N_s$ ($N_{\nu_x} + 2N_{\nu_y} \pm N_s$).

The authors wish to thank Dr L. Chen of the Institute of High Energy Physics, Beijing, People's Republic of China, for his study on optimizing the phase II lattice. They also wish to thank Dr Ando and Dr Miyahara of the SPring-8 Project Team for their special encouragement, and Professor Kamitsubo for his encouragement as well as for providing the chance to study this problem.

References

Autin, B. & Marti, Y. (1973). CERN ISR-MA/73-17. CERN, Geneva, Switzerland.

Brunelle, P., Level, M. P., Nadji, A., Sommer, M., Zyngier, H., Nghiem, P., Payet, J. & Tkatchenko, A. (1994). *Proc. EPAC94*, London, UK, pp. 615–617. Singapore: World Scientific.

Farvacque, L. & Ropert, A. (1989). ESRF-SR/LAT-89-15. ESRF, Grenoble, France.

Joho, W., Marchand, P., Rivkin, L. & Streun, A. (1994). *Proc. EPAC94*, London, UK, pp. 627–629. Singapore: World Scientific.

Kaltchev, D., Servranckx, R. V., Craddock, M. K. & Joho, W. (1995). *Proc. PAC95*, Dallas, USA, pp. 2823–2825. Piscataway, NJ: IEEE.

Kamitsubo, H. (1991). *Nucl. Instrum. Methods*, **A303**, 421–434.

Kamiya, Y. & Kihara, M. (1983). National Laboratory for High Energy Physics, KEK 83-16. Tsukuba, Japan.

Kamiya, Y., Koseki, T., Kudo, H., Nagatsuka, T., Shinoe, K., Takaki, H., Haga, K., Honda, T., Hori, Y., Izawa, M., Kasuga, T., Kobayashi, H., Kobayashi, Y., Nakamura, N., Takiyama, Y., Tobiyama, M., Sato, Y. & Sasaki, S. (1994). *Proc. EPAC94*, London, UK, pp. 639–641. Singapore: World Scientific.

Sands, M. (1970). *The Physics of Electron Storage Rings: an Introduction*. Springfield, VA: National Technical Information Service.

Sommer, M. (1983). Report LAL/RT/83-15. Laboratoire de l'Accelerateur Lineaire, Univerité de Paris-Sud, 91405 Orsay, France.

Takaki, H., Kobayashi, Y., Matsuda, K. & Kamiya, Y. (1995). *Proc. PAC95*, Dallas, USA, pp. 281–283. Piscataway, NJ: IEEE.

Tanaka, H., Kumagai, N. & Tsumaki, K. (1992). *Nucl. Instrum. Methods*, A**313**, 529–545.

Teng, L. C. (1985). Argonne National Laboratory, LS-17. Argonne, IL, USA.

Tsumaki, K., Nagaoka, R., Tanaka, H., Yoshida, Y. & Hara, M. (1989). *Proc. 7th Symp. Accel. Sci. Technol.*, pp. 290–292. Research Center for Nuclear Physics, Osaka University, Japan.